Driving Forces in the Delivery of Penetratin Conjugated G Protein Fragment

Stefania Albrizio,[§] Laura Giusti,[⊥] Gerardino D'Errico,[†] Cinzia Esposito,[▽] Francesca Porchia,[⊥] Gabriella Caliendo,[§] Ettore Novellino,[§] Maria R. Mazzoni,[⊥] Paolo Rovero,[‡] and Anna M. D'Ursi*[,▽]

Departments of Chemistry and Pharmaceutical and Toxicological Chemistry, University of Naples "Federico II", I-80131 Naples, Italy, Department of Pharmaceutical Sciences, University of Salerno, I-84084 Fisciano, Italy, Laboratory of Peptide and Protein Chemistry and Biology, University of Florence, I-50019 Sesto Fiorentino, Italy, and Department of Psychiatry, Neurobiology, Pharmacology and Biotechnology, University of Pisa, Pisa, Italy

Received August 2, 2006

A42 is a chimera peptide consisting of $G\alpha_s(374\text{-}394)C^{379}A$—the 21-mer C terminus of the $G\alpha_s$ protein, able of adenosine inhibitory activity—and penetratin—the 16 residue fragment, derived from the homeodomain of the *Drosophila* transcription factor *Antennapedia*. A42 is able to cross cell membranes and to inhibit A_{2A} and A_{2B} adenosine and β-adrenergic receptor stimulated camps (D'Ursi et al. *Mol. Pharmacol*. **2006**, *69*, 727−36). Here we present an extensive biophysical study of A42 in different membrane mimetics, with the objective to evaluate the molecular mechanisms which promote the membrane permeation. Fluorescence, CD, and NMR data were acquired in the presence of negatively charged and zwitterionic sodium dodecyl sulfate and dodecylphosphocholine surfactants. To validate the spectroscopic results in a larger scale, fluorescence microscopy experiments were performed on negatively charged and zwitterionic dipalmitoylphosphatidylglycerol and dipalmitoylphosphatidylcholine vesicles. Our results show that the internalization of A42 is mainly driven by electrostatic interactions, hydrophobic interactions playing only a secondary, sinergistic role. The distribution of the charges along the molecule has an important role, highlighting that internalization is a process which requires a specific matching of peptide and membrane properties.

Introduction

The discovery of an increasing number of new molecular targets endowed with therapeutic potential has recently raised the interest of the researchers on the specificity of ligands acting as modulators. In this respect, peptides and proteins are considered with growing interest because their three-dimensional structural complexity is responsible for a new attracting type of specificity. However, the therapeutic use of peptides and protein is hampered by the poor permeability of the plasma membrane which prevents the cellular uptake of large and hydrophilic molecules. Electroporation, microinjection, and liposome internalizations are techniques used to achieve intracellular delivery of peptides and proteins. Unfortunately, these methods, whenever effective in vitro and for research purposes, have demonstrated limited therapeutic application due to their toxicity and immunogenicity.[1] An alternative strategy[2] is based on the fusion of therapeutic peptides or proteins to short peptide sequences able to cross the cell membrane. These molecules, named "cell-penetrating peptides" (CPPs),[3−12] are amphiphilic peptides, which can be internalized by cells via mechanisms that require low energy and are receptor mediated or not. Penetratin[12] —a 16 residue fragment derived from the homeodomain of the *Drosophila* transcription factor *Antennapedia*—has been the most thoroughly studied among CPPs, and it is used in a great number of drug delivery applications.

G protein coupled receptors (GPCRs) are considered excellent drug targets for new molecules, due to their partecipation in numerous pathophysiological pathways. Large molecular libraries are screened for the molecular ability to act at the GPCR receptorial level as agonists or antagonists.[13−14] As an alternative approach, GPCRs were recently considered as targets for polypeptides able to block coupling between the receptor and the G protein intracellularly and derived from the putative contact surface of either the receptor or the G protein.[15−19] In particular, due to the essential role of the C-terminal portion of the G protein α subunit, to realize the coupling between the G protein and the cognate receptor, peptides derived from the C terminus of $G\alpha^a$ subunits have been successfully used to mimic the whole G protein in the transduction.[20−23] We recently demonstrated that several peptides corresponding to the C terminus of the $G\alpha_s$ subunit were able to inhibit the agonist binding to the A_{2A} adenosine receptor.[24−26] In particular, the 21-mer residues, $G\alpha_s(374\text{-}394)C^{379}A$, was shown to be the most effective, offering a therapeutic potential to modulate the A_{2A} adenosine receptor, directly affecting the transduction process at an intracellular level.[27] The peptide (dubbed) A42 is a chimera peptide consisting of the CPP penetratin and the 21-mer $G\alpha_s$ protein C-terminal fragment ($G\alpha_s(374\text{-}394)C^{379}A$). It was

* Corresponding author. Phone: +39-089-969748. Fax: +39-089-962828. E-mail: dursi@unisa.it.
§ Department of Pharmaceutical and Toxicological Chemistry, University of Naples "Federico II".
⊥ University of Pisa.
† Department of Chemistry, University of Naples "Federico II".
▽ University of Salerno.
‡ University of Florence.

[a] Abbreviations: Gα, the α subunit of heterotrimeric G proteins; G_s, a G protein linked with the activation of adenylyl cyclase; $G\alpha_s$, the α subunit of G_s; $G\alpha_s(374\text{-}394)C^{379}A$, a synthetic peptide corresponding to those residues of $G\alpha_s$ with a cysteine substituted by an alanine (a Gα subunit followed by numbers refers to the corresponding peptide); NMR, nuclear magnetic resonance; CD, circular dichroism; CF, carboxy-fluoresceinated; CMC, critical micellar concentration; FMOC, 9-fluorenylmethoxycarbonyl; HPLC, high-performance liquid chromatography; DQF-COSY, double quantum filtered correlated spectroscopy; TOCSY, total correlated spectroscopy; NOESY, nuclear Overhauser enhancement spectroscopy; NOE, nuclear Overhauser effect; MD, molecular dynamics; MLV, multilamellar lipid vescicles; GTPγS, guanosine-5′-*O*-(3-thiotriphosphate); SDS, sodium dodecyl sulfate; DPC, dodecylphosphocholine; DPPG, dipalmitoylphosphatidylglycerol; DPPC, dipalmitoylphosphatidylcholine; SAR, structure−activity relationship; 1D, 2D, and 3D, one-, two-, and three-dimensional. Abbreviations used for amino acids and designation of peptides follow the rules of the IUPAC-IUB Commission of Biochemical Nomenclature in *J. Biol. Chem.* **1972**, *247*, 977−983. Amino acid symbols denote L-configuration unless indicated otherwise.

10.1021/jm060935b CCC: $37.00
Published on Web 03/10/2007

designed and synthesized in our lab, and it was demonstrated to be able to cross HMEC-1 and PC12 cell plasma membranes and to inhibit A_{2A} and A_{2B} adenosine and β-adrenergic receptor stimulated camps.[28] A preliminary NMR investigation, carried out in SDS micelle solution, provided information on A42 secondary structure. Penetratin and the cargo portion—Gα$_s$(374−394)C^{379}A—as constituents of the chimera peptide assumed α-helical structure, preserving the conformational preferences of the free fragments.

How CPP peptides and CPP conjugated peptides could be able to interact with plasma membrane, pursuing the delivery of biological molecules inside the cell, is an open question. Some hypotheses claim that the main forces driving the internalization process vary accordingly to the chemical nature of the CPP sequence—basic, amphiphilic, hydrophobic. Other theories suppose that the permeation of plasma membrane is uniquely dependent on electrostatic interactions between the CPPs and the phosphates of the cell surface.[29−30] In addition, the presence of lipid rafts and heparan sulfate rich regions[31−33] highlights the role of the membrane composition as the platform driving different and specific forms of delivery.

The present work aims to clarify the molecular mechanism driving the delivery of penetratin conjugated Gα$_s$—A42—across the membrane. We performed a biophysical analysis of A42 in different membrane mimicking systems, by using a combined methodological approach. To evaluate the relevance of the electrostatic or hydrophobic forces as potential driving factors of membrane permeation, we collected data in membrane mimicking environments characterized by different electrostatic and hydrophobic properties. Consistently, fluorescence, CD, and NMR data were acquired in the presence of negatively charged and zwitterionic SDS and DPC micelles. To validate the spectroscopic results in a larger scale, fluorescence microscopy experiments were performed on negatively charged and zwitterionic DPPG and DPPC vesicles.

Experimental Section

Peptide Synthesis. Peptides were synthesized by the continuous-flow solid-phase method using Fmoc chemistry on a Milligen 9050 automatic synthesizer. Crude peptides were purified by reverse-phase HPLC on a preparative Vydac C_{18} column (2.2 × 25 cm) using a 15−30% gradient of acetonitrile in 0.1% trifluoroacetic acid water (v/v). Analytical data have been reported elsewhere.[28]

Fluorescence Titration Measurements. Peptide−surfactant interactions were studied by monitoring the changes in the Trp fluorescence emission spectra with increasing surfactant concentrations. Fluorescence measurements were performed at 300 K using an LS 55 luminescence spectrofluorimeter (Perkin-Elmer). The excitation wavelength was 280 nm, and emission spectra were recorded between 310 and 450 nm, at slit widths of 5 nm. Titrations were performed by adding known amounts of an aqueous solution containing the peptide (~10^{-6} M) and the surfactant at a concentration well above the CMC to a weighed amount of an aqueous solution of the peptide at the same concentration, initially put into the spectrofluorimetric couvette. By this procedure the surfactant concentration was progressively increased, while the peptide concentration remained constant during the whole titration. After each addition, 20 min were given to let equilibrium be reached. Titrations were performed on the conjugated peptide with SDS and DPC; for comparison, the measurements were also performed on penetratin with the same surfactants.

Circular Dichroism Spectroscopy. CD experiments were performed on an 810-Jasco spectropolarimeter, using a quartz cuvette with a path length of 1 mm. CD spectra of the peptide in water were measured at 5 °C intervals from 5 to 30 °C and at a pH range from 4 to 7. The peptide was dissolved in deionized water and diluted to arrive at a final concentration of 40 μM (concentration was estimated from the UV absorption spectra; molar absorpitivities of 5560 M^{-1} cm^{-1} and 1200 M^{-1} cm^{-1}, at 280 nm, for Triptophan and Tyrosine, respectively, were applied). To study the interaction of the peptide with both the monomeric and micellar forms of SDS and DPC surfactants, titration of the peptide aqueous solution was performed by adding known amounts of DPC and SDS concentrated solutions containing the peptide at the same concentration of the titrated solution. By this procedure, the surfactant concentration was progressively increased, while the peptide concentration remained constant during the whole titration. Mean residues ellipticities were calculated using the equation obsd/*lcn*, where obsd is ellipticity measured in degrees, *l* is the length of the cell in centimeters, *c* is the peptide concentration in mol/liter, and *n* is the number of amino acid residues in the peptide. As a preliminary part of CD investigation, in order to exclude possible transmission problems at high energy, absorption spectra of all the examined solutions in the same range investigated by CD (190−260 nm) were performed,[34] obtaining values of the total absorbance (peptide + surfactant + solvent + cell) lower than 0.1. CD spectra were the average of 10 accumulations from 190 to 260 nm, recorded with a bandwidth of 1 nm, at scanning speed of 50 nm/min. The instrument was calibrated with (+)-10-camphorsulfonic acid at 290 nm. During all the measurements, the trace of the High Tension voltage was checked to be less than 700 V, which should ensure reliability of the obtained data.[34] Base lines of either solvent or micellar solutions without peptide were subtracted from each respective sample to yield the contribution.

NMR Spectroscopy. Samples for NMR spectroscopy were prepared by dissolving the appropriate amount of A42 in water/DPC solution (pH ≈ 5) to obtain a concentration of 1 mM peptide and 100 mM DPC.

NMR spectra were recorded on a Bruker DRX-600 spectrometer. One-dimensional (1D) NMR spectra were recorded in the Fourier mode with quadrature detection and the water signal was suppressed by low-power selective irradiation in the homogated mode. DQF-COSY, TOCSY, and NOESYexperiments were run in the phase-sensitive mode using quadrature detection in ω_1 by time-proportional phase incrementation of the initial pulse.[35−39]

Data block sizes comprised 2048 addresses in t_2 and 512 equidistant t_1 values. Before Fourier transformation, the time domain data matrices were multiplied by shifted $\sin^2$ functions in both dimensions. A mixing time of 70 ms was used for the TOCSY experiments. NOESY experiments were run at 300 K with mixing times in the range of 100−250 ms. The qualitative and quantitative analysis of DQF-COSY, TOCSY, and NOESY spectra were obtained using the SPARKY interactive program package.[40]

Structure Calculation. Peak volumes were translated into upper distance bounds with the CALIBA routine of the DYANA software.[41] The necessary pseudoatom corrections were applied for nonstereospecifically assigned protons at prochiral centers and for the methyl group. After discarding redundant and duplicated constraints, the final list of constraints (198 intraresidue and 114 interresidue constraints in DPC) were used to generate an ensemble of 200 structures by the standard protocol of simulated annealing in torsion angle space implemented in DYANA. No dihedral angle restraints and no hydrogen bond restraints were applied.

The refinement of the structures was performed by in vacuo minimization using the Discover module of MSI InsightII 2000 software, using the cvff force field and applying a dielectric constant value of 1**r*.[42] The structures were relaxed, first constrained and then unconstrained by using a combination of steepest descent and conjugate gradients minimization algorithms until the maximum rms derivative was less than 0.01 kcal/Å.

Molecular dynamics procedures on peptide side chains were carried out keeping the backbone geometry fixed. After an equilibration period of 10 ps, during which temperature was gradually increased from 10 to 300 K, molecular dynamics simulations were run at 300 K for 600 ps. In the course of the molecular dynamics frame structures were saved each 10 fs.

The final structures, analyzed using the InsightII 2000 program,[42] were deposited in the PDB and are now publicly accessible. PDB

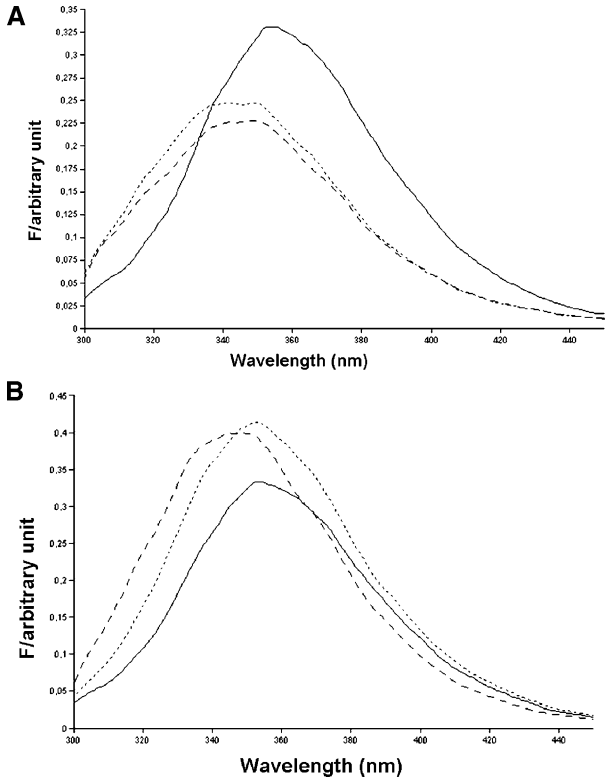

Figure 1. Tripthophan emission spectra (range 300−450 nm) of A42 in the presence of SDS (A) and DPC (B) surfactants. The spectra are recorded in aqueous buffer phosphate (continuous line) at premicellar (dotted line) or micellar (dashed line) surfactant concentrations.

ID codes for the models in SDS and in DPC micelles are 2O00 and 2NZZ, respectively. Computations were performed on an SGI Octane computer.

Fluorescence Microscopy. Fluorescence microscopy experiments were carried out as reported by Harishchandran and Nagaraj.[43] Multilamellar lipid vesicles (MLVs) were prepared from lipid (DPPC or DPPG) solution which was dried, desiccated, and hydrated in a phosphate buffer (pH 7) overnight. MLVs in the presence of CF labeled peptides were prepared adding CF labeled peptides at a concentration of 40 μM (lipid to peptide molar ratio 50:1) and incubating the solutions for at least 30 min. A total of 15 μL of each solution, in the presence or absence of the CF labeled peptides, was taken and spotted on a cover slip. The vesicles were imaged using a Zeiss Axioplan 2 microscope.

Results

Fluorescence Titration Measurements. The fluorescence intensities of some vibronic fine structures in the Trp fluorescence spectrum show strong environmental dependence. In particular, the emission maximum shifts from 350 to 329 nm when going from water to an apolar medium, such as dioxane. The quantum yield could also undergo large changes, whose direction and extent depend on the system under consideration.[44,45]

Fluorescence spectra were recorded on conjugated penetratin (A42) and, for comparison, on the single penetratin. Both peptides in water show Trp emission spectra typical of the aqueous environment, indicating that both Trps are exposed to the solvent medium. In Figure 1 the Trp emission spectra of A42 in water and in the presence of premicellar and micellar concentrations of SDS and DPC surfactants are shown. The addition of SDS to A42 dramatically changes the spectrum, whose maximum shifts to lower values (Figure 1A). This shift is evident also in solution in which the SDS concentration is

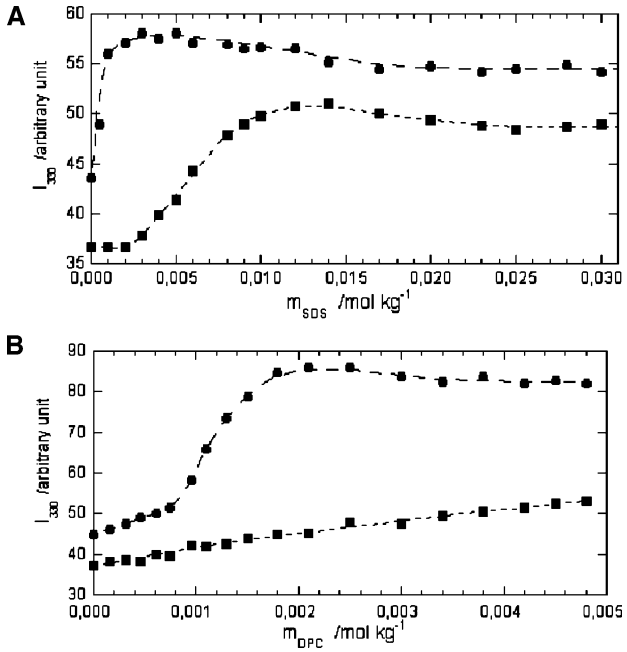

Figure 2. A42 (full circles) and penetratin (full squares) Trp fluorescence intensities (329 nm) plotted as a function of SDS (A) and DPC (B) concentrations.

lower than the CMC (0.008 M). A closer look at Figure 2A, where the Trp fluorescence intensities at 329 nm are plotted as a function of SDS concentration, shows that the spectrum change occurs almost with the first surfactant addition (i.e., at a surfactant concentration much lower than the CMC) in solutions in which micelles are absent. It is interesting to compare this behavior with that observed for penetratin with the same surfactant. In that case, the spectrum does not change appreciably up to a surfactant concentration (0.003 M), which in any case is significantly lower than the CMC (0.008 M). In the case of DPC, A42 spectrum in premicellar surfactant solution presents the same maximum as in water, see Figure 1B.

Inspection of Figure 2B shows that the addition of DPC to the conjugated peptide does not change the spectrum up to a surfactant concentration of 0.001 M, coinciding with the surfactant CMC, and the maximum tends to shift weakly to lower values. Addition of DPC to penetratin does not alter its spectrum over the whole considered surfactant concentration range.

A quantitative analysis of these data can be done according to the models which we discussed in a recent paper.[46] In the case of DPC, interaction of A42 with the surfactant occurs only at concentrations at which micelles are present. In other words, it can be described in terms of a partition coefficient[47] of the peptide between the aqueous medium and the micelles, whose value was found to be 3×10^5. In contrast, penetratin does not appear to interact with DPC micelles. In the case of SDS the peptides can induce surfactant aggregation. In particular, the association of A42 with SDS occurs also with surfactant monomers and can be described in terms of a binding coefficient (3×10^9) between the peptide and three surfactant monomers. In the case of penetratin a lower binding coefficient was found (4×10^2) with a larger number of SDS molecules ($\sim$9).[48]

Circular Dichroism Spectroscopy. A screening of the conformational preferences of A42 as a function of the environment was performed by means of CD spectroscopy. CD spectra were recorded in water at several different pH and temperature conditions (see Experimental Section). The spectrum in water does not appear to be affected by pH and temperature, and it

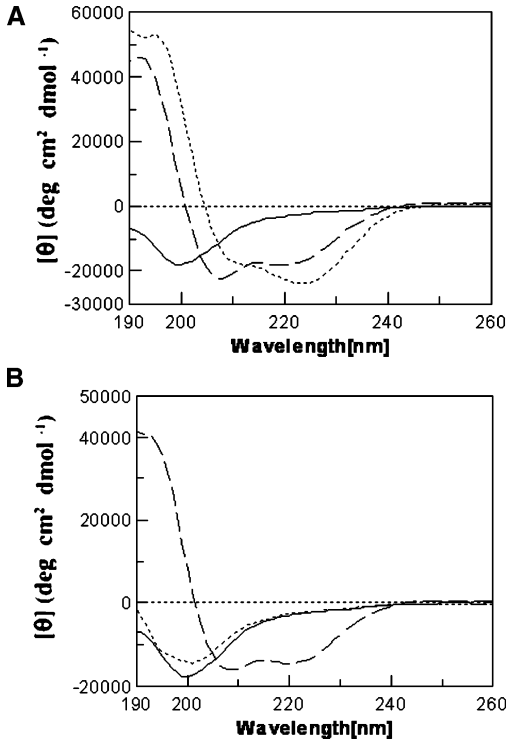

Figure 3. CD spectra of A42 in the presence of SDS (A) and DPC (B). The spectra are recorded in water (continuous line) at premicellar (dotted line) or micellar (dashed line) surfactant concentrations.

has the typical shape of a random coil structure, presenting a negative band at 201 nm (Figure 3). The CD spectra of A42 recorded in SDS and DPC micelles show the double-well shape typical of a right-handed α-helical structure including negative bands at 208 and 222 nm and an additional positive signal at 192 nm.

CD spectra of A42 were recorded in the presence of variable amounts of SDS and DPC surfactants. Whereas A42 in the presence submicellar DPC concentration is in random coil conformation, in the presence of SDS monomers assume turn-helical structures. Nevertheless, CD spectrum of A42 recorded in the presence of SDS monomers is slightly shifted toward red values and presents a weakly different shape as compared to that recorded in the presence of SDS micelles. The shift could be related to a change of the polarity of the environment in which the peptide is embedded.[49] However, the evident change in the line shape suggests some change in the peptide conformation, even if the α-helical structure remains dominant.

NMR Spectroscopy. 1D and 2D protonic spectra were recorded in an aqueous solution of 100 mM DPC concentration. Complete proton resonance assignments were achieved with the Wuthrich procedure.[50] The systematic analysis of DQF-COSY, TOCSY, and NOESY[35−39] experiments was carried out using the SPARKY software package.

The proton chemical shifts and the chemical shift indexes of A42 in DPC micelles solutions are reported in the Supporting Information.[51,52] Most of the residues of A42 in DPC micellar solutions show upfield shifts of the Hα resonances and, consequently, can be considered involved in helical structure. The analysis of the NOE connectivities relative to A42 in DPC micelles (Figure 4) evidences the presence of several medium range NOEs, in particular α-N(i, i+2), N−N(i, i+2), α-N(i, i+3), N−N(i, i+3). These contacts involve the residues of the N-terminal and the central portion of the peptide, whereas a limited number of structurally significant NOE connectivities

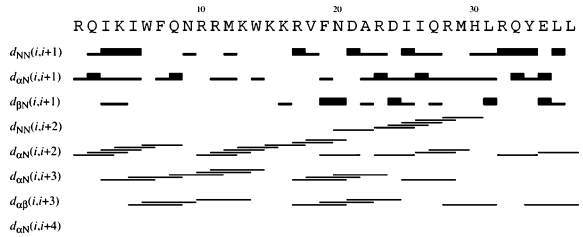

Figure 4. Sequential and medium range NOE connectivities of A42 in DPC micellar solution (80 mM), collected at NMR 600 MHz, 300 K.

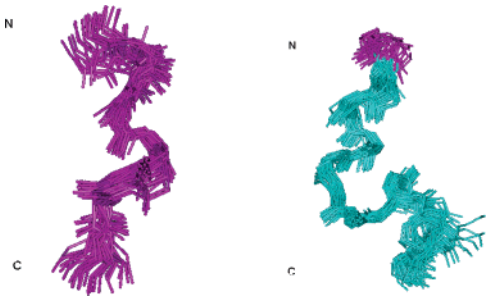

Figure 5. Superimposition of A42 NMR structures as derived from data collected in DPC micellar solution at 600 MHz and 300 K. The structures were calculated by DYANA software and overlapped at the level of backbone heavy atoms of residues 3−10 (left) and 16−29 (right). PDB ID: 2NZZ.

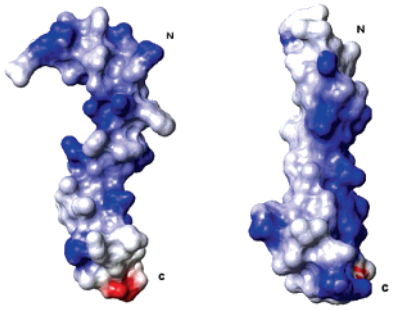

Figure 6. Molecular electrostatic potential maps of the A42 structure, obtained in SDS (left) and DPC (right) micelles. Positive, neutral, and negative potentials are colored blue, white, and red, respectively.

is observable in the C-terminal extremity of the peptide. Accordingly, we can suppose that the N-terminus and the central part of A42 assume turn-helical conformations, whereas in the C-terminal region it is characterized by random coil structures.

Structure Calculation. The structure calculation was carried out by simulated annealing in torsion angle space and restrained molecular dynamics methods based on 312 NOE-derived restraints, using the DYANA software package.[41] One set of 200 structures was generated; among them the 50 with the lowest values of target function were selected for a thorough structural analysis.

The best structures judged according to their value of target function were relaxed, using the Discover module of InsightII [MSI], first constrained, using the DYANA derived restraints, and then unconstrained. The results of structure show that a prevalence of ordered structures, in particular turn-helical conformations, is observable in correspondence of residues 3−10 and 16−29 (Figure 5), whereas the peptide proves flexible and unfolded in the C-terminal region.

Charge Distribution. The electrostatic potential surfaces using the SDS- and the DPC-bound conformation of A42 were computed using the MOLMOL program.[53] The greatest difference in the two structures is the location of the positive potential

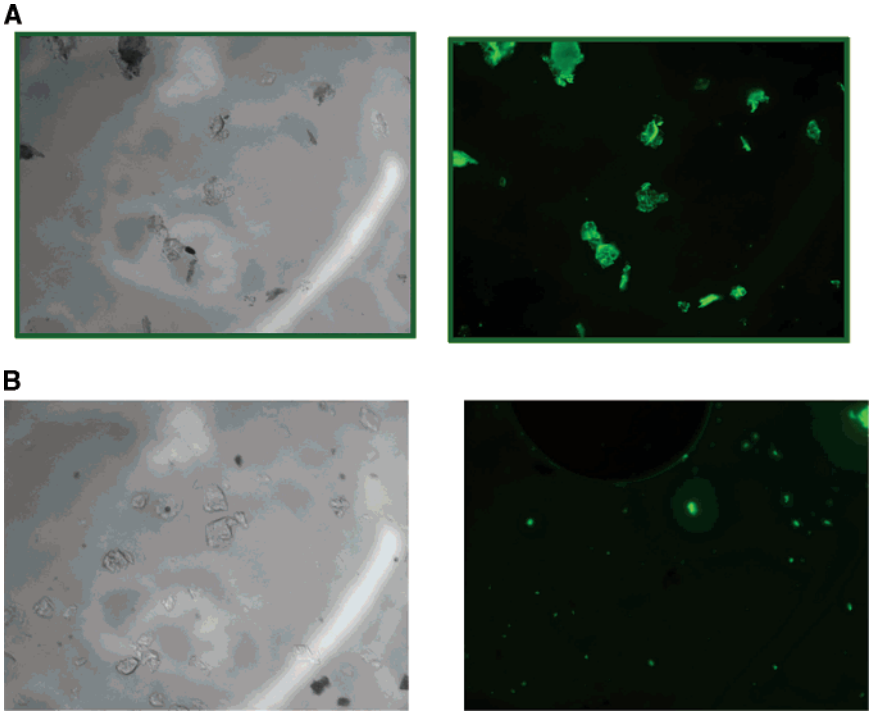

Figure 7. Detection of peptide translocation in vesicles by fluorescence microscopy. Imaged under bright field (left) and fluorescent images (right) of DPPG vesicles in presence of CF labeled A42 (panel A) and CF labeled $G\alpha_s$(374-394) (panel B).

along the A42 backbone (Figure 6). The charge distribution in DPC shows a neutral face that is definitely opposite to a positively charged one. On the contrary, in SDS the positive potential is spread out uniformly along the whole molecule.

Fluorescence Microscopy. In order to investigate the peptide translocation rate into membranes, A42 and the 21-mer $G\alpha_s$ protein C-terminal fragment were labeled at the N-terminus with CF and their localization in MLV was observed by fluorescence microscopy. As shown in Figure 7, fluorescence in the inner bilayers of DPPG vesicles incubated with CF labeled A42 is clearly observable (Figure 7A); on the contrary, DPPG vesicles incubated with the CF labeled $G\alpha_s$(374-394) did not show any fluorescence. These data further highlight the fact that penetratin is essential for the translocation of $G\alpha_s$(374-394) into the membranes. Zwitterionic DPPC vesicles proves only weakening fluorescent when incubated with CF-A42 (data not shown), supporting the importance of the negative charge to the A42 internalization.

Discussion

The understanding of the molecular mechanisms driving the internalization of hydrophilic molecules across the membrane is still questioned. A common agreement is that the process involves both electrostatic and hydrophobic interactions as the main driving forces. Our analysis of A42—the penetratin conjugated $G_s\alpha$(374-394)—in different membrane-mimicking environments aims to assess the relevance of these two factors as driving forces of membrane permeation. NMR, fluorescence, and CD data were collected in anionic SDS and zwitterionic DPC micelle systems. In order to validate the spectroscopic results on a larger scale, we monitored A42's delivery capability by fluorescence microscopy using the carboxy-fluoresceinated derivative of A42 in the presence of both anionic and zwitterionic DPPG and DPPC vesicles.

Fluorescence and CD spectra highlight a remarkable tendency of A42 to interact with negatively charged SDS surfactants. Data recorded at different SDS concentrations show the ability of the peptide to bind not only SDS micelles but also SDS monomers. Interestingly, this is unique behavior, even compared to penetratin, which proves to be affected only by micellar concentrations of surfactant. This specific behavior could be dependent on the additional positive side chains carried by the $G\alpha_s$ cargo region of A42, so suggesting that the penetratin delivery capability—and CPPs in general—could vary according to the chemical nature of the cargo molecules.

CD data show that both SDS and DPC micellar environments are able to induce A42 conformational transition from random coil to turn-helical structures. The collection of CD spectra in the presence of increasing amounts of surfactants permits the monitoring of the conformational transition. In particular, whereas DPC is effective to promote ordered A42 conformations only as micelles, SDS displays a helical inducing effect even as monomers. High-resolution NMR models of A42 indicate that, although apparently both DPC and SDS micelle systems induce folded conformations, they in fact influence the conformational properties of the peptide in a different way. The helical structure in the presence of SDS is well defined, and it is divided in two segments corresponding to the penetratin and $G_s\alpha$ sequences, respectively. On the contrary, in DPC micelles, A42 is overall characterized by an appreciable flexibility; a helical segment is evident, but it is shorter, as compared to that in SDS, and includes several different residues, located in the central region of the peptide.

The above-reported data can be interpreted, supposing that in the presence of SDS surfactants a strong electrostatic interaction takes place between the negative sulfate heads of SDS and the positively charged residues of the peptide. SDS is preferentially electrostatically attracted by the peptide which acts as an aggregation center for the surfactant molecules; consequently, the interaction among the SDS molecules is effective to form the micelles only at higher surfactant concentrations. It is reasonable that in this process the high charge density of sulfate heads is determinant.[54] The role of sulfate moieties in several biological processes, as particular component

of specific cell membrane regions, has recently been highlighted. An interaction between the penetratin conjugated peptide and the sulfate rich membrane region can be a key event for the delivery of molecules inside the cells. These interactions could occur on a biological platform, characterized by sulfate rich membrane regions which operate as specific entrance sites.

The details of penetratin-conjugated SDS interaction can be better understood through the analysis of A42 electrostatic potential maps. The molecular surfaces of the peptide according to the SDS NMR structure prove to be characterized by a spot distribution of hydrophobic and positively charged sites. This particular charge distribution suggests that multiple electrostatic contacts, between the penetratin conjugated peptide and the SDS negative moieties, can synergically lead to the membrane destabilization. Interestingly, this step can be considered the starting event in the delivery process. These hypotheses are further supported by fluorescence microscopy data, which evidenced the capability of A42 to penetrate negatively charged membrane models.

The interaction between A42 and the zwitterionic surfactant is not as effective as that with SDS. DPC molecules interact preferentially with other DPC molecules rather than with peptide itself. Consequently in a first step the micelles are formed, and successively the interaction between A42 and the micellar surface takes place. Due to the presence of zwitterionic heads of the surfactants, the A42-DPC interactions are characterized by a low electrostatic contribution, being mainly driven by a hydrophobic component. The calculation of the electrostatic potential maps relative to the NMR structure of A42 in DPC shows that the single helical stretch is amphypathic and exhibits an apolar opposite to a positively charged face. Microscopy data show that the interaction of A42 with zwitterionic DPPC vesicles does not permit the internalization of the peptide. Accordingly, we can hypothesize that in the absence of net negative charges, the interaction between the hydrophobic A42 α-helix surface and the zwitterionic DPPC vesicles, results in the neighboring of the peptide to the membrane compartment, but it is not effective to destabilize the interface and to deliver the peptide into the internal compartment.

Overall, our results show that the internalization of A42 is mainly driven by electrostatic interactions, hydrophobic interactions playing only a secondary and possibly sinergistic role. However, a particular distribution of the charges along the molecule is required, highlighting that internalization is a process involving a specific matching of peptide and membrane properties.

Supporting Information Available: Chemical shift assignments and chemical shift indexes of A42 in DPC micelle solution. This material is available free of charge via the Internet at http://pubs.acs.org.

References

(1) Zorko, M.; Langel, U. Cell-penetrating peptides: mechanism and kinetics of cargo delivery. *Adv. Drug Delivery Rev.* **2005**, *57*, 529−545.

(2) Borghouts, C.; Kunz, C.; Groner, B. Current strategies for the development of peptide-based anti-cancer therapeutics. *J. Pept. Sci.* **2005**, *11*, 713−726.

(3) Thorén, P. E. G.; Persson, D.; Esbjörner, E. K.; Goksör, M.; Lincoln, P.; Nordén, B. Membrane binding and translocation of cell-penetrating peptides. *Biochemistry* **2004**, *43*, 3471−3489.

(4) Brattwall, C. E. B.; Lincoln, P.; Norden, B. Orientation and conformation of cell-penetrating peptide penetratin in phospholipid vesicle membranes determined by polarized-light spectroscopy. *J. Am. Chem. Soc.* **2003**, *125*, 14214−14215.

(5) Lindberg, M.; Biverstahl, H.; Graeslund, A.; Maeler, L. Structure and positioning comparison of two variants of penetratin in two different membrane mimicking systems by NMR. *Eur. J. Biochem.* **2003**, *270*, 3055−3063.

(6) Magzoub, M.; Eriksson, L. E. G.; Graslund, A. Comparison of the interaction, positioning, structure induction and membrane perturbation of cell-penetrating peptides and non-translocating variants with phospholipid vesicles. *Biophys. Chem.* **2003**, *103*, 271−288.

(7) Schwarze, S. R.; Dowdy, S. F. In vivo protein transduction: intracellular delivery of biologically active proteins, compounds and DNA. *Trends Pharmacol. Sci.* **2000**, *21*, 45−48.

(8) Lindgren, M.; Hallbrink, M.; Prochiantz, A.; Langel, U. Cell-penetrating peptides. *Trends Pharmacol. Sci.* **2000**, *21*, 99−103.

(9) Lundberg, P.; Langel, U. A brief introduction to cell-penetrating peptides. *J. Mol. Recognit.* **2003**, *16*, 227−233.

(10) Fernandez-Carneado, J.; Kogan, M. J.; Pujals, S.; Giralt, E. Amphipatich peptides and drug delivery. *Biopolymers* **2004**, *76*, 196−203.

(11) Javar, P.; Langel, U. The use of cell-penetrating peptides as a tool for gene regulation. *Drug Discovery Today* **2004**, *9*, 395−402.

(12) Derossi, D.; Joliot, A. H.; Chassaing, G.; Prochiantz, A. The third helix of the Antennapedia homeodomain translocates through biological membranes. *J. Biol. Chem.* **1994**, *269*, 10444−10450.

(13) Lundstrom, K. Structural genomics of GPCRs. *Trends Biotechnol.* **2005**, *2*, 103−8.

(14) Lee, D. K.; George, S. R.; O'Dowd, B. F. Continued discovery of ligands for G protein-coupled receptors. *Life Sci.* **2003**, *74*, 293−7.

(15) Shuttleworth, S. J.; Connors, R. V.; Fu, J.; Liu, J.; Lizarzaburu, M. E.; Qiu, W.; Sharma, R.; Wanska, M.; Zhang, A. J. Design and synthesis of protein superfamily-targeted chemical libraries for lead identification and optimization. *Curr. Med. Chem.* **2005**, *12*, 1239−81.

(16) Covic, L.; Gresser, A. L.; Talavera, J.; Swift, S.; Kuliopulos, A. Activation and inhibition of G protein-coupled receptors by cell-penetrating membrane-tethered peptides. *Proc. Natl. Acad. Sci. U.S.A.* **2002**, *99*, 643−8.

(17) Chang, M.; Zhang, L.; Tam, J. P.; Sanders-Bush, E. Dissecting G protein-coupled receptor signaling pathways with membrane-permeable blocking peptides. Endogenous 5-HT(2C) receptors in choroid plexus epithelial cells. *J. Biol. Chem.* **2000**, *275*, 7021−9.

(18) Hawes, B. E.; Luttrell, L. M.; Exum, S. T.; Lefkowitz, R. J. Inhibition of G protein-coupled receptor signaling by expression of cytoplasmic domains of the receptor. *J. Biol. Chem.* **1994**, *269*, 15776−15785.

(19) Feldman, D. S.; Zamah, A. M.; Pierce, K. L.; Miller, W. E.; Kelly, F.; Rapacciuol, A.; Rockman, H. A.; Koch, W. J.; Luttrell, L. M. Selective inhibition of heterotrimeric Gs signaling. Targeting the receptor-G protein interface using a peptide minigene encoding the Gα$_s$ carboxyl terminus. *J. Biol. Chem.* **2002**, *277*, 28631−28640.

(20) Gilchrist, A.; Bunemann, M.; Li, A.; Hosey, M. M.; Hamm, H. E. A dominant-negative strategy for studying roles of G proteins in vivo. *J. Biol. Chem.* **1999**, *274*, 6610−6616.

(21) Kisselev, O. G.; Meyer, C. K.; Heck, M.; Ernst, O. P.; Hofmann, K. P. Signal transfer from rhodopsin to the G-protein, evidence for a two-site sequential fit mechanism. *Proc. Natl. Acad. Sci. U.S.A.* **1999**, *96*, 4898−4903.

(22) Rasenick, M. M.; Watanabe, M.; Lazarevic, M. B.; Hatta, S.; Hamm, H. E. Synthetic peptides as probes for G proten function, carboxyl-terminal Gα$_s$ peptides mimic G$_s$ and evoke high affinity agonist binding to β-adrenergic receptors. *J. Biol. Chem.* **1994**, *269*, 21519−21525.

(23) Hamm, H. E.; Deretic, D.; Arendt, A.; Hargrave, P. A.; Konig, B.; Hofmann, K. P. Site of G protein binding to rhodopsin mapped with synthetic peptides from the α subunit. *Science* **1988**, *241*, 832−835.

(24) Albrizio, S., D'Ursi, A. M.; Fattorusso, C.; Galoppini, C.; Greco, G.; Mazzoni, M. R.; Novellino, E.; Rovero, P. Conformational studies on a synthetic C-terminal fragment of the α-subunit of G$_s$ proteins. *Biopolymers* **2000**, *54*, 186−194.

(25) D'Ursi, A. M.; Albrizio, S.; Greco, G.; Mazzeo, S.; Mazzoni, M. R.; Novellino, E.; Rovero, P. Conformational analysis of the Gα protein C-terminal portion. *J. Pept. Sci.* **2002**, *8*, 576−588.

(26) Grieco, P.; Albrizio, S.; D'Ursi, A. M.; Giusti, L.; Mazzoni, M. R.; Novellino, E.; Rovero. P. A Structure-Activity Relationship Study on Position-2 of the Gα$_s$ C-Terminal Peptide Able to Inhibit G$_s$ Activation by A$_{2A}$ Adenosine Receptor. *Eur. J. Med. Chem.* **2003**, *38*, 13−18.

(27) Mazzoni, M. R.; Taddei, S.; Giusti, L.; Rovero, P.; Galoppini, C.; D'Ursi, A. M.; Albrizio, S.; Triolo, A.; Novellino, E.; Greco, G.; Lucacchini, A.; Hamm, H. E. A Gα$_s$ carboxyl-terminal peptide prevents G$_s$ activation by the A$_{2A}$ adenosine receptor. *Mol. Pharmacol.* **2000**, *58*, 226−236.

(28) D'Ursi, A. M.; Giusti, L.; Albrizio, S.; Porchia, F.; Esposito, C.; Caliendo, G.; Gargini, C.; Novellino, E.; Lucacchini, A.; Rovero, P.; Mazzoni, M. R. A Membrane-Permeable Peptide Containing the Last 21 Residues of the $G\alpha_s$ Carboxyl Terminus Inhibits G_s-Coupled Receptor Signaling in Intact Cells: Correlations between Peptide Structure and Biological Activity. *Mol. Pharmacol.* **2006**, *69*, 727−36.
(29) Futaki, S.; Suzuki, T.; Ohashi, W.; Yagami, T.; Tanaka, S.; Ueda, K.; Sugiura, Y. Arginine-rich peptides. An abundant source of membrane-permeable peptides having potential as carriers for intracellular protein delivery. *J. Biol. Chem.* **2001**, *276*, 5836−40.
(30) Wender, P. A.; Mitchell, D. J.; Pattabiraman, K.; Pelkey, E. T.; Steinman, L.; Rothbard, J. B. The design, synthesis, and evaluation of molecules that enable or enhance cellular uptake: peptoid molecular transporters. *Proc. Natl. Acad. Sci. U.S.A.* **2000**, *97*, 13003−8.
(31) Fittipaldi, A.; Ferrari, A.; Zoppe, M.; Arcangeli, C.; Pellegrini, V.; Beltram, F.; Giacca, M. Cell membrane lipid rafts mediate caveolar endocytosis of HIV-1 Tat fusion proteins. *J. Biol. Chem.* **2003**, *278*, 34141−9.
(32) Wadia, J. S.; Stan, R. V.; Dowdy, S. F. TAT-HA fusogenic peptide enhances escape of TAT-fusion proteins after lipid raft macropinocytosis. *Nat. Med.* **2004**, *10*, 310−5.
(33) Foerg, C.; Ziegler, U.; Fernandez-Carneado, J.; Giralt, E.; Rennert, R.; Beck-Sickinger, A. G.; Merkle, H. P. Decoding the entry of two novel cell-penetrating peptides in HeLa cells: lipid raft-mediated endocytosis and endosomal escape. *Biochemistry* **2005**, *44*, 72−81.
(34) Kelly, S. M.; Jess, T. J.; Price, N. C. How to study proteins by circular dichroism. *Biochim. Biophys. Acta* **2005**, *1751*, 119−139.
(35) Piantini, U.; Soerensen, O. W.; Ernst, R. R. Multiple quantum filters for elucidating NMR coupling networks. *J. Am. Chem. Soc.* **1982**, *104*, 6800−6801.
(36) Braunschweiler, L.; Ernst, R. R. Coherence transfer by isotropic mixing: application to proton correlation spectroscopy. *J. Magn. Reson.* **1983**, *53*, 521−528.
(37) Bax, A.; Davis, D. G. Mlev-17-based two-dimensional homonuclear magnetization transfer spectroscopy. *J. Magn. Reson.* **1985**, *65*, 355−360.
(38) Macura, S.; Ernst, R. R. Elucidation of cross relaxation in liquids by two-dimensional NMR spectroscopy. *Mol. Phys.* **1980**, *41*, 95−117.
(39) Jeener, J.; Meyer, B. H.; Bachman, P.; Ernst, R. R. Investigation of exchange processes by two-dimensional NMR spectroscopy. *J. Chem. Phys.* **1979**, *71*, 4546−4553.
(40) Goddard, T. D.; Kneller, D. G. *SPARKY 3 NMR software*; University of California, San Francisco, 2001.
(41) Guntert, P.; Mumenthaler, C.; Wüthrich, K. Torsion angle dynamics for NMR structure calculation with the new program DYANA. *J. Mol. Biol.* **1997**, *273*, 283−298.
(42) MSI Molecular Symulations, 965 Scranton Road, San Diego, CA 92121−3752.
(43) Harishchandran, A.; Nagaraj, R. Interaction of a pseudosubstrate peptide of protein kinase C and its myristoylated form with lipid vesicles: only the myristoylated form translocates into the lipid bilayer. *Biochim. Biophys. Acta* **2005**, *1713*, 73−82.
(44) Ambrosone, L.; D'Errico, G.; Ragone, R. Interaction of tryptophan and N-acetyltryptophanamide with dodecylpentaoxyethyleneglycol ether micelles. *Spectrochim. Acta A* **1997**, *53*, 1615−1620.
(45) Callis, P. R.; Liu, T. Quantitative prediction of fluorescence quantum yields for tryptophan in proteins. *J. Phys. Chem. B* **2004**, *108*, 4248−4259.
(46) Esposito, C.; D'Errico, G.; Armenante, M. R.; Giannecchini, S.; Bendinelli, M.; Rovero, P.; D'Ursi, A. M. Physicochemical characterization of a peptide deriving from the glycoprotein gp36 of the feline immunodeficiency virus and its lipoylated analogue in micellar systems. *Biochim. Biophs. Acta* **2006**, *58*, 1653−61.
(47) Nernst, W. Verteilung eines stoffes zwishen zwei löungsmitteln und zwishen lösungsmittel und dampfraum. *Z. Phys. Chem.* **1891**, *8*, 110−139.
(48) Christiaens, B.; Symoens, S.; Verheyden, S.; Engelborghs, Y.; Joliot, A.; Prochiantz, A.; Vandekerckhove, J.; Rosseneu, M.; Vanloo, B. Tryptophan fluorescence study of the interaction of penetratin peptides with model membranes. *Eur. J. Biochem.* **2002**, *269*, 2918−2926.
(49) Chen, Y.; Wallace, B. A. Secondary solvent effects on the circular dichroism spectra of polypeptides in non-aqueous environments: influence of polarisation effects on the far ultraviolet spectra of Alamethicin. *Biophys. Chem.* **1997**, *65*, 65−74.
(50) Wüthrich, K. *NMR of Proteins and nucleic acids*; John Wiley & Sons, Inc.: New York, 1986; p 320.
(51) Wishart, D. S.; Sykes, B. D.; Richards, F. M. Relationship between Nuclear Magnetic Resonance chemical shift and protein secondary structure. *J. Mol. Biol.* **1991**, *222*, 311−333.
(52) Wishart, D. S.; Sykes, B. D.; Richards, F. M. The chemical shift index. A fast and simple method for the assignment of protein secondary structure trough NMR spectroscopy. *Biochemistry* **1992**, *31*, 1647−1651.
(53) Koradi, R.; Billeter, M.; Wütrich, K. MOLMOL: a program for display and analysis of macromolecular structures. *J. Mol. Graphics* **1996**, *14*, 51−55.
(54) Huibers, P. D. T. Quantum-chemical calculations of the charge distribution in ionic surfactants. *Langmuir* **1999**, *15*, 7546−7550.

JM060935B